

# Polymeric nanospheres as a displacement fluid in enhanced oil recovery

Luky Hendraningrat · Julien Zhang

Received: 18 December 2014 / Accepted: 31 December 2014 / Published online: 11 January 2015  
© The Author(s) 2015. This article is published with open access at Springerlink.com

**Abstract** This paper presents the investigation of using nanoscale polyacrylamide-based spheres (nanospheres) as a displacement fluid in enhanced oil recovery (EOR). Coreflood experiments were conducted to evaluate the impact of nanospheres and its concentration dispersed in model formation water on oil recovery during a tertiary oil recovery process. The coreflood results showed that nanospheres can enhance residual oil recovery in the sandstone rock samples and its concentration showed a significant impact into incremental oil. By evaluating the contact angle, it was observed that wettability alteration also might be involved in the possible oil displacement mechanism in this process together with fluid behavior and permeability to water that might divert injected fluid into unswept oil areas and enhance the residual oil recovery. These investigations promote nanospheres aqueous disperse solution as a potential displacement fluid in EOR.

**Keywords** Enhanced oil recovery · Polyacrylamide · Nanospheres · Coreflood · Displacement mechanism

## Introduction

The nanotechnology is now chosen as an alternative method to unlock the remaining oil resources and applied as a new enhanced oil recovery (EOR) method in last

decade (Ju et al. 2006; Ogolo et al. 2012; Miranda et al. 2012; Roustaei et al. 2012; Hendraningrat et al. 2013a; Hendraningrat and Torsæter 2014a, b). Das et al. (2008) defined “Nano” as one billionth ( $10^{-9}$ ) in science term and nanofluids as suspensions of nanoparticles in base fluids (include saline water, oil, bio-fluids, polymer solutions, etc.). The nanoparticles are defined as zero-dimensional building blocks of nanomaterial form. Nanospheres are spherical form and based on three-dimensional linked polyacrylamide ranging from  $10^1$  to  $10^3$  nm.

Polyacrylamide (PAM) is a class of long-chain synthetic polymers and a water-soluble polymer (Bell 2005). It has a chemical formula of  $C_3H_5NO$ , as showed in Fig. 1. In industries, PAM is most frequently used as water management or wastewater treatment because it has ability to increase the viscosity of water by creating a thicker solution and encourage flocculation of particles present in water (IHS 2014). In oil and gas industries, PAM is generally used in drilling fluids as additive (IHS 2014). In China, the application of PAM has the highest segment for EOR currently (IHS 2014). In addition, polymeric microspheres and nanospheres have been applied as water mobility control both as a pilot and full-field, and showed fantastic results in reducing water cut, increasing sweep efficiency and improving oil recovery (Yuan et al. 2010; Li et al. 2012; Tian et al. 2012). They reported that polymeric microspheres and nanospheres can swell when meet with water and then reduce water permeability due to its ability of reducing the capillary force and change water flow path. Consequently water goes into bypassed area and enhances displacement efficiency. Tian et al. (2012) also reported that polymeric microspheres and nanospheres have some advantages such as no degradation at high temperature and salinity. However, the impact of this polymeric microspheres and nanospheres to wettability alteration of rock is

L. Hendraningrat (✉)  
Department of Petroleum Engineering and Applied Geophysics,  
Norwegian University of Science and Technology (NTNU),  
Trondheim, Norway  
e-mail: lucker83@gmail.com

J. Zhang  
ZJ Green Energy Co., Ltd, Zhengzhou, China

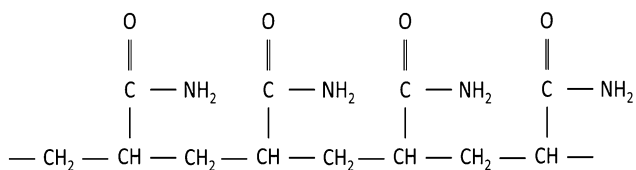


**Fig. 1** Chemical formula of polyacrylamide

not reported yet. The main aim of this research is to investigate the impact of polymeric nanospheres dispersed in model formation water in oil recovery during a tertiary oil recovery (EOR) process at different concentration and reveal possible displacement mechanism through contact angle experiment, filtration mechanism and rheological behavior analyses.

## Experiments

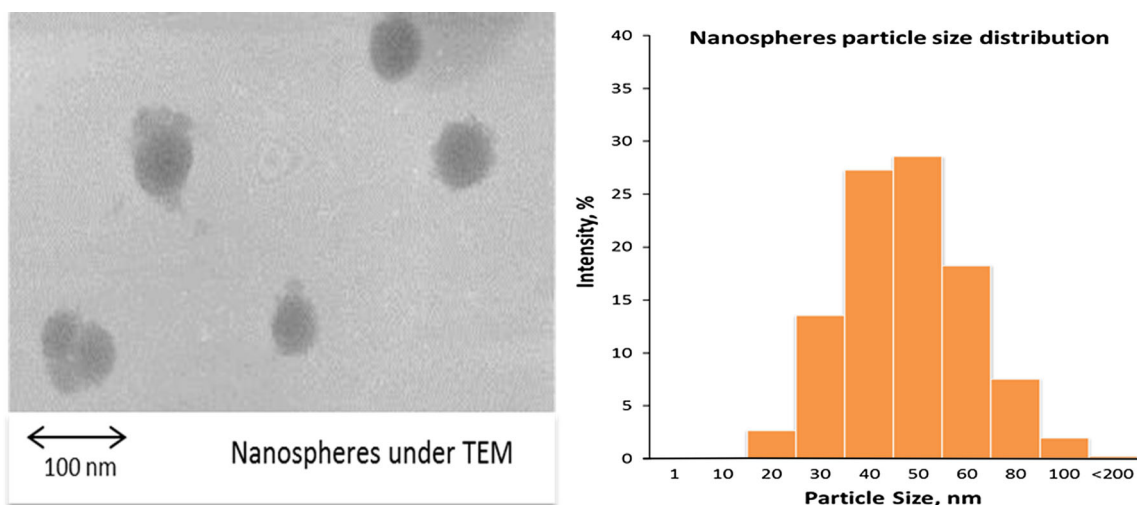
### Fluids

A liquid of nanoscale polyacrylamide-based spheres (nanospheres) was acquired from ZL-EOR Chemicals Ltd. Model formation brine from sodium chloride (30,000 ppm) was used in this experiment. Based on particle size characterization using transmission electron microscopy (TEM) and Malvern nanosizer as shown in Fig. 2, it has average diameter in between 20 and 200 nm. Nanospheres at different concentrations were synthesized using model formation brine with a weight concentration ranged from 0.01 to 0.1 wt%. The concentration of nanospheres is expressed in terms of mass percentage (wt%) which represents the weight of nanospheres respect to the weight of the

dispersing fluid. Those concentrations were chosen based on our study in silica-based nanofluid (Hendraningrat et al. 2013b). Later, nanofluid (nanospheres dispersed in model formation brine) was prepared using high-speed magnetic stirring for 5–10 min and then sonicated with ultra-sonication at 60–100 % amplitude (output power 90–100 W) at similar duration. A degassed light crude oil from a field at North Sea was used as base oleic phase in this experiment. The properties of the various fluids are presented in Table 1.

### Core samples preparation and characterization

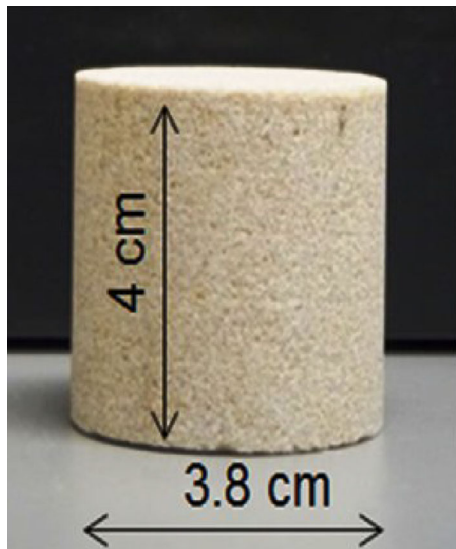
As representative reservoir rock, Berea sandstone outcrop cores were employed in this experiment (Fig. 3). Potts and Kuehne (1988) mentioned some preferential benefits of using Berea sandstone core in laboratory coreflooding experiments such as uniform rock properties, commercially available and inexpensive. In addition, Berea sandstone also covers a wide range of porosity and permeability. In this experiment, the range of porosity and permeability is 17–18 % and 80–100 mD, respectively. Based on our measurement using sister cores through Amott–Harvey wettability index measurement, the original wetting system of employed core samples is strongly water wet (SWW) with wettability index ranging from +0.7 to +0.9. Energy-dispersive X-ray (EDX) and X-ray diffraction (XRD) were performed for mineralogy characterization. The selected sister cores were dominated by quartz (83–93 %), alkali feldspar (6–8 %), and pyroxene (<1 %). The initial water saturation ( $S_{wi}$ ) ranged from 25 to 34 % which is typical for Berea sandstone. Craig (1971) reported that the characteristics of  $S_{wi}$  for strongly water-wet (SWW) cores are



**Fig. 2** Nanospheres characterization and particle distribution

**Table 1** Properties of fluids at room condition

Fluid type	Composition	TDS (ppm)	Density (g/cm <sup>3</sup> )	Viscosity (cP)
Model formation water	Distilled water + NaCl 3.0 wt%	30,000	1.0220	1.001
PAM-1	Model form. brine + nanospheres 0.01 wt%	–	1.0071	1.073
PAM-2	Model form. brine + Nanospheres 0.05 wt%	–	1.0173	1.123
PAM-3	Model form. brine + nanospheres 0.1 wt%	–	1.0144	1.093
Crude oil	–	–	0.8260	5.1

**Fig. 3** Berea sandstone core samples

typically greater than 20–25 % PV because water fills the small pores and forms a thin water film over the rock surfaces in a water-wet system. Consequently, the  $S_{wi}$  for water-wet systems is relatively high. Meanwhile, the variation of  $S_{wi}$  values at similar wettability may be caused by core cleaning and handling methods (Anderson 1987; Bobek et al. 1958; Grist et al. 1975).

#### Coreflood procedure

The two-phase oil–water system coreflood instrument was set up as shown in Fig. 4. The Hassler core cell was placed in a heating cabinet, but the displacement tests were performed at room temperature. The sleeve pressure and injection rate were maintained at 20 bar and 0.2 cm<sup>3</sup>/min respectively, during the displacement processes. The injection rate was selected to approximate typical reservoir velocities. The displacement tests were performed in sequential flooding. During the first cycle of the forced imbibition process, SSW (denoted as WF1) was injected at a PV between 4 and 5 into the core

plugs until oil production stopped or 100 % water cut (WC). Thus, residual oil saturation ( $S_{or}$ ) was established due to waterflooding (WF1). The nanospheres were then injected as the next cycle at a range of 3–4 PV as a tertiary recovery process (denoted as NF). Re-injected (secondary) SSW (denoted as WF2) was performed as a post-nanoflooding cycle at a range of 4–5 PV to selected cores. The expelled oil from a core was recorded and measured in a two-phase glass separator during the displacement processes. The water production (effluent) was collected in a water accumulator. A camera was installed to record the oil recovery during the displacement processes. A differential pressure transmitter (range of 0–30 bar) was connected to the inlet and outlet ends of the core cell to measure and record the pressure drop across the core during the flooding processes.

#### Contact angle measurement

The contact angle of the crude oil/brine/rock (COBR) system was measured directly on transparent quartz plates using a Goniometry KSV CAM instrument at ambient conditions (Fig. 5). A series of rectangular transparent plates of quartz were used as the solid substrates in this study. Each quartz plate has average dimensions of 2.8 cm in length, 1.5 cm in width and 0.19 cm in height. The quartz plates were first cleaned with a detergent solution and rinsed with methanol followed by distilled water. The plates were dried in a heating cabinet at 50–60 °C for 3–5 days. The original wettability of the quartz plate was observed by measuring the contact angle between brine and crude oil and is considered as water wet. Meanwhile crude oil is treated as the oleic phase and nanofluid as the aqueous phase, as shown in Fig. 6. The measured drop shape was fitted by the formula as follows:

$$\theta = \cos^{-1} \left( \frac{\sigma_s - \sigma_{sl}}{\sigma_l} \right) \quad (1)$$

where  $\sigma$  describes the interfacial tension components of phase, indices  $s$  and  $l$  stand for solid and liquid (water or oil) phases and  $\theta$  is the contact angle.

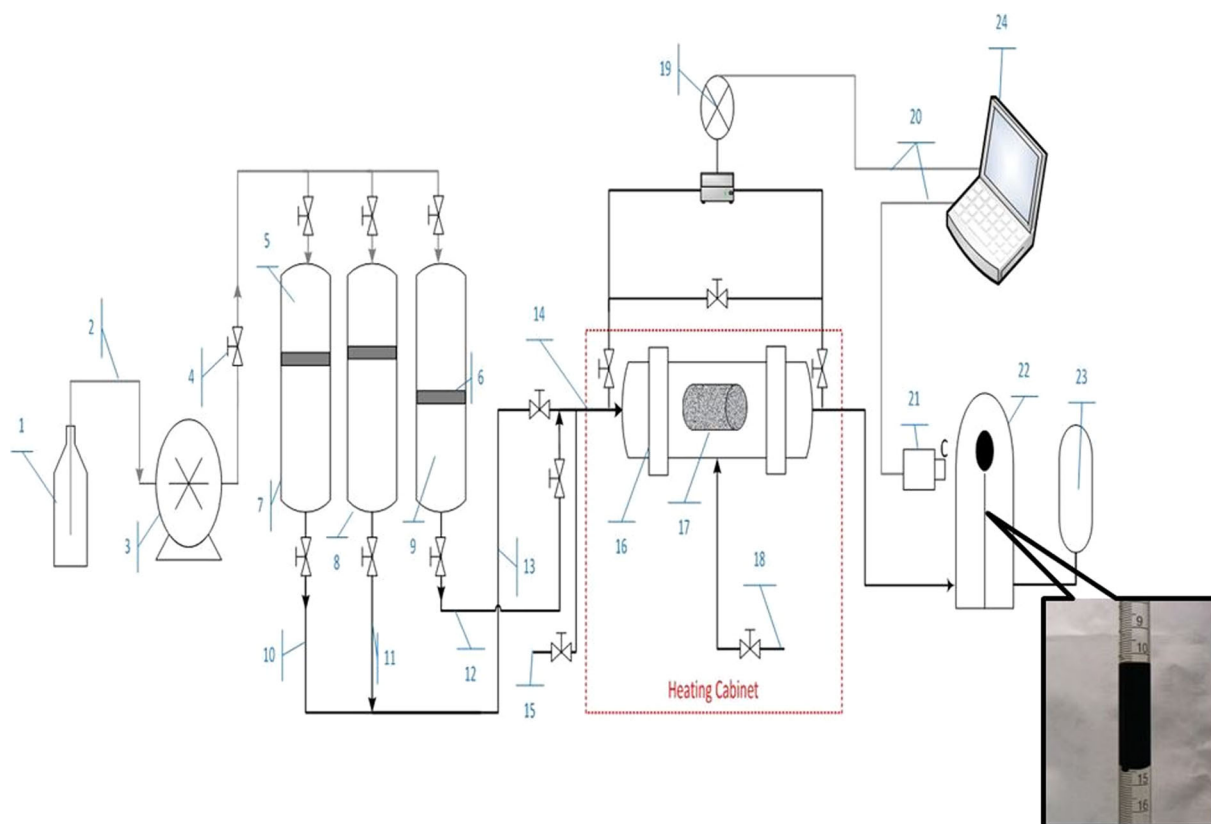


**Fig. 4** Experimental setup schematic. 1 Pump fluid (Exxol D60), 2 injection pipe (ID 1.5 mm), 3 pump, 4 valve, 5 pump fluid in vessel-A, 6 piston plate, 7 SSW in vessel-A, 8 nanofluid in vessel-B, 9 crude oil in vessel-C, 10 SSW pipeline, 11 nanofluid pipeline, 12 oil pipe, 13 water-phase pipeline, 14 inlet pipeline, 15 bypass valve, 16 Hassler

core cell inside oven, 17 core plug inside cell, 18 sleeve pressure, 19 pressure transmitter, 20 connection cable to PC, 21 camera recorder, 22 oil–water separator, 23 water accumulator, 24 computer/PC as controller and data acquisition

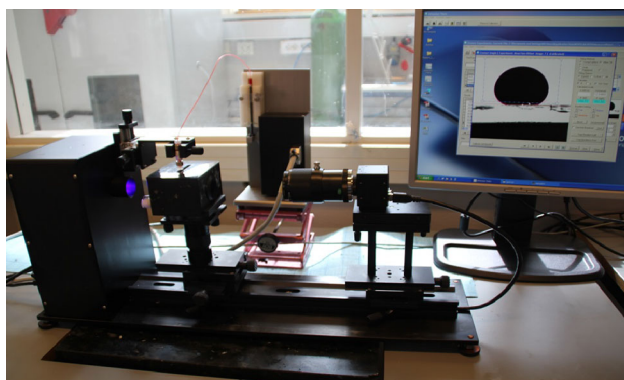


**Fig. 5** Contact angle measurements using the Goniometry KSV CAM instrument

Treiber et al. (1971) defined the contact angle in a 3-phase system (water, oil and rock) as follows: water wet in a range from  $0^\circ$  to  $75^\circ$ , intermediate/neutral wet from  $75^\circ$  to  $105^\circ$  and oil wet from  $105^\circ$  to  $180^\circ$ . A zero contact

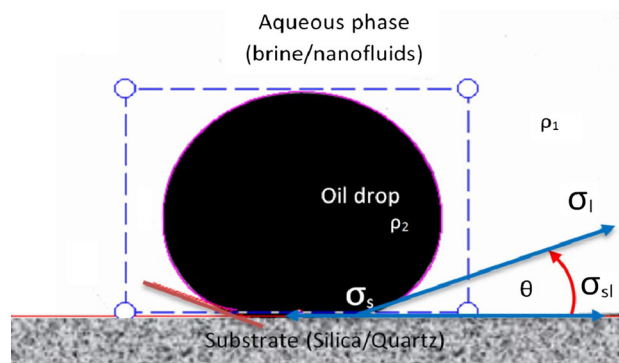


**Fig. 6** Contact angle formation on polished quartz plate between crude oil and aqueous phase

angle indicates that the denser fluid completely wets the solid. Treiber et al. (1971) also reported that a water-advancing contact angle is relevant in the waterflooding process.

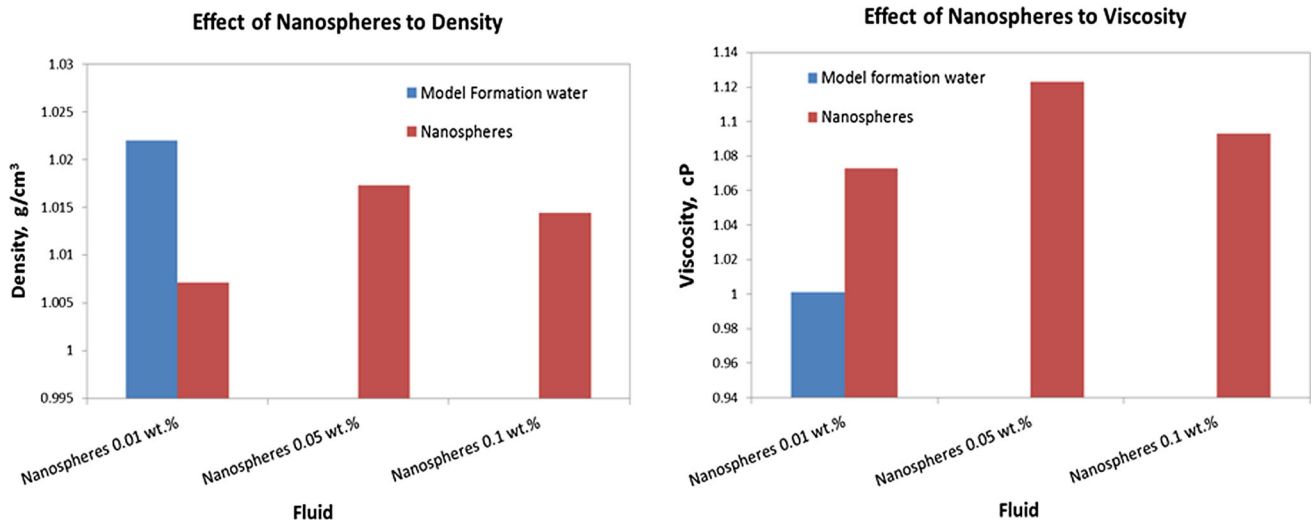


Fig. 7 Effect of nanospheres to fluid properties

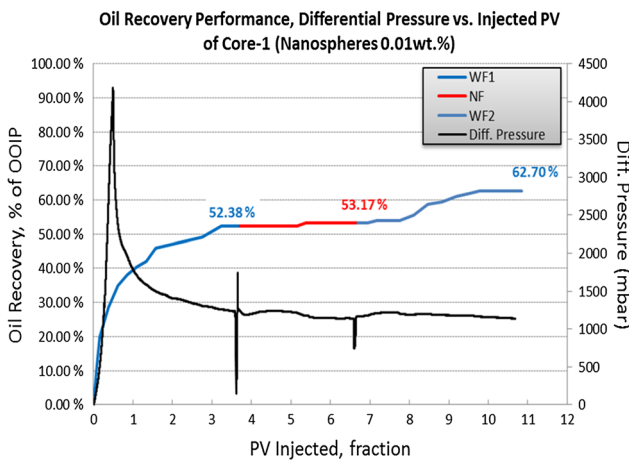


Fig. 8 Oil recovery profile each sequence vs. differential pressure of Core-1 (nanospheres 0.01 wt%)

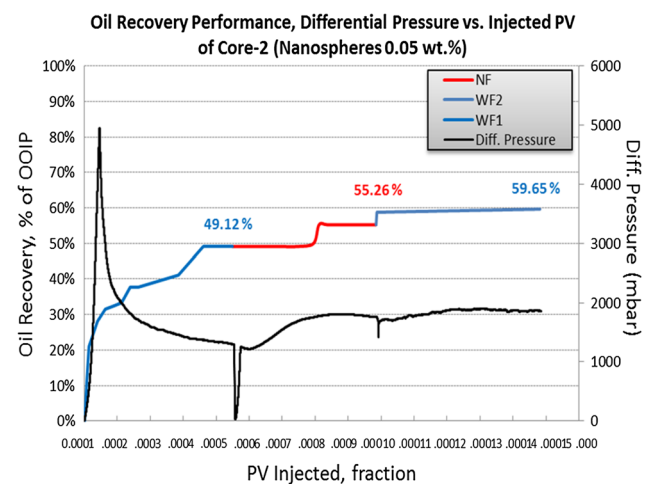


Fig. 9 Oil recovery profile each sequence vs. differential pressure of Core-2 (nanospheres 0.05 wt%)

**Results and discussion**

**Fluid properties**

Basic fluid properties of nanospheres, such as density and viscosity, have been measured by varying its concentrations and compared with model formation water. Based on our measurements, experimental results showed that nanospheres dispersed in model formation brine have different rheological behaviors, as shown in Fig. 7. Introducing nanospheres into model formation brine slightly decreases density and increases the viscosity. However, increasing its concentration does not give any specific trend both into density and viscosity. It is observed that the influence of nanospheres in terms of density is low with deviation in range between 0.5 and 1.5 % with respect to model formation water. Meanwhile, it did not significantly influence

viscosity which increased from 1 cp to 1.08–1.12 cp with respect to model formation water. Hydrolyzed polyacrylamide (HPAM) is most often used in industries to increase viscosity of water by creating a thicker solution and encourage flocculation of particles present in water (due to intermolecular winding), PAM-based nanospheres behave differently from HPAM in this respect.

**Coreflood experiment**

The displacement experimental results for each sequence (WF1, NF and WF2) and the corresponding pressure drop profiles are plotted in Figs. 8, 9 and 10. In the first waterflooding sequence (WF1), model formation water that consists of sodium chloride (30,000 ppm) was injected until achieving 100 % water cut (WC) through the Berea

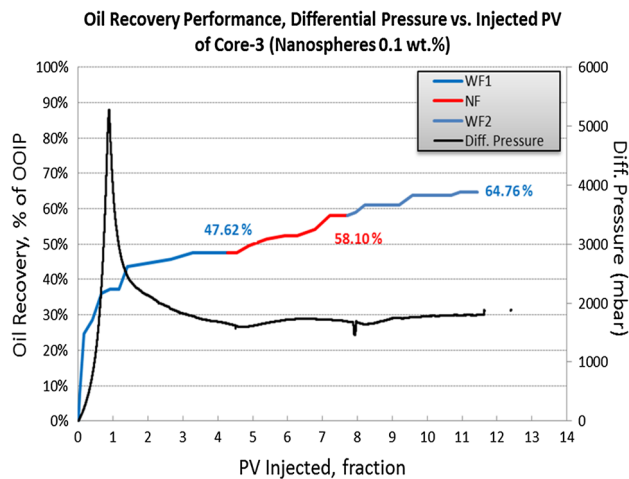


**Fig. 10** Oil recovery profile each sequence vs. differential pressure of Core-3 (nanospheres 0.1 wt%)

sandstone in all of cases studied. The oil recoveries after WF1 ranged from 47 to 52 % OOIP, and  $S_{or}$  ranged from 34 to 35 % PV. Oil recovery variations typically result from complex COBR interactions, such as the complexity of the pore structure and the distribution of the fluid in the pore spaces (Morrow 1990). However, these results are worthy to compare the NF sequence because  $S_{or}$  is quite similar among three cores.

Once the WC reached 100 % during the WF1 cycle, the nanospheres were injected as a tertiary recovery process (nanoeor, denoted as NF) as plotted in the red line in Figs. 8, 9 and 10. It successfully increased incremental oil from 1 to 10 % points of OOIP. Meanwhile, it reduced  $S_{or}$  in range between 0.6 and 7 % point of PV which has a trend that  $S_{or}$  further decreases as concentration of nanospheres increases. Similarly, the trends clearly show that additional oil recovery of the NF sequence increased as the concentration of nanospheres increased from 0.01 to 0.1 wt%. The pressure drop profile slightly increased from the WF to the NF sequence, particularly at higher concentration (e.g. 0.05 and 0.1 wt%).

In the last sequence (WF2), the model formation water was re-injected to reduce the residual oil in the cores. As shown in Figs. 8, 9 and 10, the WF2 scheme was performed on all cores; all of which lead to another increment oil in a range between 4 and 9 % points of the OOIP. Additionally, the residual oil saturation significantly decreased in a range between 3 and 7 % of the PV. The pressure drop profile of WF2 cycle is relatively similar to previous cycle (NF) in all cores.

### Displacement mechanism

The dynamic wettability modification, as assessed by contact angle measurement under ambient conditions, is shown in Fig. 11. Effect of different concentrations of nanospheres was

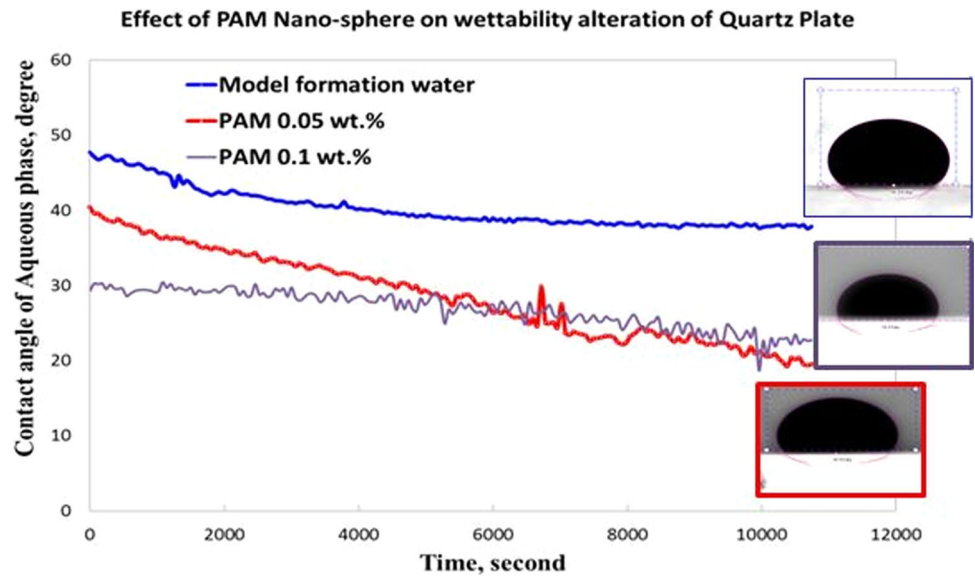
evaluated parameter during the fluid-rock interaction. Unfortunately, a case of nanospheres 0.01 wt% does not show in this report due to inconclusive result. Two other concentrations of nanospheres are provided different responses to wettability modification in water-wet quartz plate. Once the nanospheres is introduced into the model formation water and increased its concentration, the contact angle is likely reduced, which means that the nanospheres may have rendered the quartz plate toward more water wet. Hence, the surface quartz wettability may be modified and will favor the aqueous phase. Morrow (1990) reported that large changes in the wettability of a quartz surface can be achieved by adsorption of a monolayer of polar molecules. However, the use of a quartz plate has limitations in using rock surface as a single mineral (quartz), as reported by Morrow (1990).

Figure 12 shows the restriction in flow of nanospheres in Berea sandstone from observing the inlet/injection point of the cores after the displacement tests at different nanospheres concentrations. Esfahani et al. (2014) reported there are some physical factors that affect a nanoparticles transport in subsurface situation such as initial particle concentration, flow velocity, grain size and depth of porous media. Meanwhile the chemical factors are caused by ionic strength, pH and organic matter. They also reported that initial silica-based nanoparticles concentration is the key factor among physic-chemical factors above because of some mechanisms such as interaction between particles (e.g. with strong attraction forces between nanoparticles) at high concentrations and causes aggregation. Nanospheres with negative charge on the surface due to the functional groups acrylate, stay individually in water phase and have repellent force with the negative charge of sandstone. After being mixed with model formation water, nanospheres will hydrate, due to the nature of polyacrylamide, from a microscopic point of view; each nanospheres have very high viscosity (however the bulk viscosity of them dispersed in water is low). They get into pore throat where is dominated by capillary force, due to their nanoscale size, they will show Brownian movement, in doing this the water permeation is reduced. To evaluate this effect, residual retention factor (RRF) is calculated as follows (Skauge et al. 2010):

$$RRF = \frac{\Delta P_{\text{after NF}}}{\Delta P_{\text{before NF}}} \quad (2)$$

The RRF is defined as the ratio between the differential pressure after and before NF. The RRF calculation is summarized in Table 2. The higher the RRF, the higher is the nanospheres retention possibility in porous media but mobility ratio will be lower because nanospheres influence viscosity. Additionally, changing of hydrodynamic system due to nanospheres and strong attraction forces appears such as van der Waals and Brownian motion, a portion of the nanospheres was shown to have settled inside the cores

**Fig. 11** Effect of nanospheres on wettability alteration of water-wet quartz plate



**Fig. 12** Inlet point of Core-2 (nanospheres 0.05 wt%)

**Table 2** Residual retention factor calculation

Core #	Average RRF	Injected nanospheres concentration wt%
1	0.95	0.01
2	1.39	0.05
3	1.07	0.1

and created aggregation. The size of nanospheres will reach several hundred nano-size meters to several micron meters in certain days by adsorbing water (swelling). This adsorption will significantly increase water flow resistance and reduce water permeability (Al-Sharji et al. 2001). Consequently, it might divert injected fluid (during NF and WF2 cycles) into unswept oil areas (bypassed oil), in parallel with modification of the surface sand grains wettability to enhance the oil recovery.

**Concluding remarks and future work**

This study results show that polymeric nanospheres can enhance residual oil recovery in the rock samples and its concentration showed a significant impact into incremental oil. By evaluating the contact angle, it was observed that wettability alteration also might be involved in the oil displacement mechanism in this process together with reduction of mobility ratio and permeability to water that might divert injected fluid (during NF and WF2 cycles) into unswept areas (bypassed oil) and enhance the oil recovery. These investigations promote polymeric nanospheres suspension as a potential displacement fluid in EOR. Further study is required, for instance stability tests, repeat coreflood testing by increasing nanospheres concentration, and various parameter effects to EOR process such as initial wettability of rock, temperature, different salinity and salt compositions.

**Open Access** This article is distributed under the terms of the Creative Commons Attribution License which permits any use, distribution, and reproduction in any medium, provided the original author(s) and the source are credited.

**References**

Al-Sharji HH, Grattoni CA, Dawe RA, Zimmerman RW (2001) Disproportionate permeability reduction due to polymer adsorption-entanglement. Soc Pet Eng. doi:10.2118/68972-MS

Anderson WG (1987) wettability literature survey-part 6: the effects of wettability on waterflooding. JPT J Pet Technol 39(12): 1605–1622

Bell S (2005) Improved field test measures polyacrylamide fluid. Oil Gas J. Retrieved from: <http://www.ogj.com/articles/print/volume-103/issue-4/special-report/improved-field-test-measures-polyacrylamide-fluid.html>. Accessed Oct 2014

- Bobek JE, Mattax CC, Denekas MO (1958) Reservoir rock wettability-its significance and evaluation. SPE J 213:155–160
- Craig FF Jr. 1971. The reservoir engineering aspects of waterflooding. vol. 1, Monograph Series, Society of Petroleum Engineers, New York
- Retrieved from: <http://www.ihs.com/products/chemical/planning/ceh/acrylamide.aspx>. Accessed Oct 2014
- Das SK, Choi SUS, Yu W, Pradeep T (2008) Nanofluids science and technology. Wiley, Hoboken. ISBN 0470074736
- Esfahani et al (2014) Transport and retention of polymer-stabilized zero-valent iron nanoparticles in saturated porous media: effects of initial particle concentration and ionic strength. J Ind Eng Chem 20:2671–2679
- Grist DM, Langley GO, Neustadter EL (1975) The dependence of water permeability on core cleaning methods in the case of some sandstone samples. J Can Pet Technol 14(2):48–52
- Hendraningrat L, Torsæter O (2014a) Metal oxide-based nanoparticles: revealing their possibility to enhance the oil recovery at different wettability systems. Appl NanoSci. Springer. doi:10.1007/s13204-014-0305-6
- Hendraningrat L, Torsæter O (2014b) Effects of the initial rock wettability on silica-based nanofluid-enhanced oil recovery processes at reservoir temperatures. Energy Fuels 28(10):6228–6241. doi:10.1021/ef5014049
- Hendraningrat L, Li S, Torsæter O (2013a) A coreflood investigation of nanofluid enhanced oil recovery. J Petrol Sci Eng 111:128–138
- Hendraningrat L, Li S, Torsæter O (2013b) Enhancing oil recovery of low-permeability Berea sandstone through optimized nanofluids concentration. Soc Pet Eng (SPE). Paper SPE 165283-MS
- Ju B, Tailiang F, Mingxue M (2006) Enhanced oil recovery by flooding with hydrophilic nanoparticles. China Part 4:41–46
- Li X, Ying Z, Jia Y, Liu X, Yang T, Ma L (2012) Application of nanosphere deep profile control and displacement technology in Changqing oilfield. Oilfield Chem 29(4)
- Miranda CR, De Lara LS, Tonetto BC (2012) Stability and mobility of functionalized silica nanoparticles for enhanced oil recovery application. Soc Pet Eng. SPE 157033-MS
- Morrow NR (1990) Wettability and its effect on oil recovery. J Pet Tech 42(12):1476–1484. doi:10.2118/21621-PA (SPE-21621-PA)
- Ogolo NA, Olafuyi OA, Onyekanwu MO (2012) Enhanced oil recovery using nanoparticles. Soc Pet Eng. SPE 160847-MS
- Potts DE, Kuehne DL (1988) Strategy for alkaline/polymer flood design with Berea and reservoir-rock corefloods. SPERE 3(4):1143–1152. doi:10.2118/14935-PA
- Roustaei A, Saffarzadeh S, Mohammadi M (2012) An evaluation of modified silica nanoparticles' efficiency in enhancing oil recovery of light and intermediate oil reservoirs. Egypt J Pet 22(3):427–433
- Skauge T, Spildo K, Skauge A (2010) Nano-sized particles for EOR. Soc Pet Eng. doi:10.2118/129933-MS
- Tian Y, Wang L, Tang Y, Liu C, Ma C, Wang T (2012) Research and application of nano polymer microspheres diversion technique of deep fluid. Soc Pet Eng. SPE 156999-MS
- Treiber LE, Duane LE, Archer L, Owens WW (1971) A laboratory evaluation of the wettability of fifty oil-producing reservoirs. SPE J 12:531–540
- Yuan W, Liu X, Wei H, Liu J, Yang H, Hu S, Li Y, Wang D (2010) Research and application effect of polymeric microsphere in Wen-10 of Sinopec Zhongyuan Oil field. Inner Mong Petrochem 12:122